Chemistry of Metals and Alloys

Chem. Met. Alloys 10 (2017) 76-92
Ivan Franko National University of Lviv
www.chemetal-journal.org

Phase equilibria in the Ce–Ti–Sb and Gd–Ti–Sb ternary systems at 600°C and the crystal structures of the $Ce_2Ti_7Sb_{12}$ and $Gd_2Ti_{11}Sb_{14}$ compounds

Oleksandr SENCHUK[1]*, Yaroslav TOKAYCHUK[1], Roman SERKIZ[2], Pavlo DEMCHENKO[1], Roman GLADYSHEVSKII[1]

[1] *Department of Inorganic Chemistry, Ivan Franko National University of Lviv, Kyryla i Mefodiya St. 6, 79005 Lviv, Ukraine*
[2] *Scientific-Technical and Educational Centre for Low Temperature Research, Ivan Franko National University of Lviv, Drahomanova St. 50, 79005 Lviv, Ukraine*
* *Corresponding author. Tel.:* +380-32-2394506*; e-mail: senchuk91@gmail.com*

Received June 6, 2017; accepted June 27, 2017; available April 1, 2018

The phase equilibria in the Ce–Ti–Sb and Gd–Ti–-Sb ternary systems at 600°C were established by means of X-ray powder diffraction and EDX analysis. The formation of two ternary compounds in the Ce–Ti–Sb system, Ce_3TiSb_5 (Hf_5CuSn_3 type) and $Ce_2Ti_7Sb_{12}$ ($La_2Ti_7Sb_{12}$ type), and of one ternary compound in the Gd–Ti-Sb system, $Gd_2Ti_{11}Sb_{14}$ ($Sm_2Ti_{11}Sb_{14}$ type), was confirmed. At 600°C, seven binary compounds were found to exist in the Ti–Sb system, four in the Ce–Sb system, and four in the Gd–Sb system. No binary compounds form in the {Ce, Gd}–Ti systems. The crystal structures of the $Ce_2Ti_7Sb_{12}$ and $Gd_2Ti_{11}Sb_{14}$ compounds were refined on X-ray powder diffraction data, starting from the initial atomic parameters of the $La_2Ti_7Sb_{12}$ and $Sm_2Ti_{11}Sb_{14}$ structure types, respectively. The isothermal sections of the phase diagrams of the Ce–Ti–Sb and Gd–Ti–Sb ternary systems at 600°C were constructed in the whole concentration range.

Cerium / Gadolinium / Titanium / Antimony / Ternary compound / Phase diagram / Crystal structure

Introduction

The phase diagrams of the binary systems Ce–Sb and Gd–Sb are relatively well-studied [1] and characterized by the formation of a few binary compounds [2]. In the Ce–Sb system five compounds are known: Ce_2Sb, Ce_5Sb_3, Ce_4Sb_3, CeSb, and $CeSb_2$, whereas in the Gd–Sb system the compounds Gd_5Sb_3, Gd_4Sb_3, GdSb, $GdSb_2$, $Gd_{16}Sb_{39}$, and Gd_2Sb_5 have been reported. Among the latter, the $GdSb_2$ was found to exist only at high pressures and temperatures. The phase equilibria in the binary Ti–Sb system have not yet been completely investigated and there are still uncertainties in the phase diagram [1]. The crystal structures of the compounds $Ti_{3.2}Sb_{0.80}$ (Ti_4Sb), Ti_3Sb, Ti_2Sb or $Ti_{2.15}Sb_{0.85}$ (Ti_5Sb_2), Ti_5Sb_3, $Ti_{4.8}Sb_{3.29}$, $Ti_{10.84}Sb_{7.73}$, TiSb, and $TiSb_2$ have been determined [2]. Concerning the phase Ti_5Sb_8 the crystal structure has not yet been fully determined, but it is considered to belong to the tetragonal structure type $Zr_{2.6}Ti_{2.4}Sb_8$ (space group $I4_122$) [3]. The crystal structures of a few compounds of this type $(M',Ti)_5Sb_8$ (M' = Zr, Hf, Nb, Mo) have been determined from X-ray single crystal data [4] and the compound $Zr_\delta Ti_{5-\delta}Sb_8$ was found to have a significant homogeneity range with $0 \le \delta \le 3.9$ [3]. The cell parameters of binary Ti_5Sb_8 were determined from X-ray single crystal data by Bie *et al*. [5], but no other structural data have been published for this phase. Early investigations suggested the presence of a phase Ti_6Sb_5 [6]. The existence of a compound at this composition was not confirmed in later studies, but a compound with similar cell parameters was found at the composition 11:8 ($Ti_{10.84}Sb_{7.73}$) [7]. A metastable Ti_3Sb phase with hexagonal Mg_3Cd-type structure has also been reported [8]. Crystallographic data for compounds in the boundary binary systems are summarized in Table 1.

The amount of data available on the phase equilibria and the formation of compounds in the ternary systems *R*–Ti–Sb (*R* = rare-earth metal) is scarce. Up to now, isothermal sections of the phase diagrams have been constructed for only two systems (La–Ti–Sb and Er–Ti–Sb) [5], and three series of isostructural ternary compounds are known, namely R_3TiSb_5 (*R* = La-Nd, Sm) [2,9,10], $R_2Ti_7Sb_{12}$

Table 1 Crystallographic data for binary compounds reported in the Ce–Sb, Gd–Sb and Ti–Sb systems.

Compound	Structure type	Pearson symbol	Space group	Cell parameters, Å			Reference
				a	*b*	*c*	
Ce_2Sb	La_2Sb	*tI*12	*I*4/*mmm*	4.538	-	17.861	[14]
Ce_5Sb_3	Mn_5Si_3	*hP*16	*P*6$_3$/*mcm*	9.295	-	6.536	[15]
Ce_4Sb_3	Th_3P_4	*cI*28	*I*-43*d*	9.519	-	-	[16]
CeSb	NaCl	*cF*8	*Fm*-3*m*	6.416	-	-	[17]
$CeSb_2$	$SmSb_2$	*oS*24	*Cmce*	6.2807	6.1561	18.267	[15]
Gd_5Sb_3	Mn_5Si_3	*hP*16	*P*6$_3$/*mcm*	9.0173	-	6.3242	[18]
Gd_4Sb_3	Th_3P_4	*cI*28	*I*-43*d*	9.2149	-	-	[19]
GdSb	NaCl	*cF*8	*Fm*-3*m*	6.2178	-	-	[20]
$GdSb_2$ hp1-ht	$SmSb_2$	*oS*24	*Cmce*	6.157	5.986	17.83	[21]
$GdSb_2$ hp2-ht	$HoSb_2$	*oS*6	*C*222	3.296	5.93	8.03	[21]
$Gd_{16}Sb_{39}$	$Gd_{16}Sb_{39}$	*mS*124	*C*2/*m*	57.395	4.151 β = 99.21°	13.209	[22]
Gd_2Sb_5	Dy_2Sb_5	*mP*28	*P*2$_1$/*m*	13.1747	4.1864 β = 102.485°	14.7521	[23]
Ti_3Sb	Cr_3Si	*cP*8	*Pm*-3*n*	5.2228	-	-	[24]
Ti_3Sb tetr. [a]	Ti_3Sb	*tI*32	*I*4/*mcm*	10.465	-	5.2639	[6]
Ti_2Sb	Ti_2Sb	*tI*16-4	*I*4/*mmm*	3.9546	-	14.611 [b]	[25]
Ti_5Sb_3	Yb_5Sb_3	*oP*32	*Pnma*	10.2182	8.3432	7.1748	[26]
$Ti_{4.8}Sb_{3.3}$	Ti_5Ga_4	*hP*18	*P*6$_3$/*mcm*	7.982	-	5.515	[27]
$Ti_{10.84}Sb_{7.73}$	$Cr_{11}Ge_8$	*oP*76	*Pnma*	14.6228	5.5972	17.644	[7]
TiSb	NiAs	*hP*4	*P*6$_3$/*mmc*	4.123	-	6.265	[28]
Ti_5Sb_8	$Zr_{2.6}Ti_{2.4}Sb_8$	*tI*52	*I*4$_1$22	6.492	-	26.514	[5]
$TiSb_2$	$CuAl_2$	*tI*12	*I*4/*mcm*	6.660	-	5.818	[29]

[a] possibly stabilized by Al or Si, *cf.* $Ti_5Sb_{1.7}Si_{1.3}$, *a* = 10.346(2), *c* = 5.152(1) Å [30]; [b] at 150 K

(*R* = La-Nd) [2,5] and $R_2Ti_{11}Sb_{14}$ (*R* = Sm, Gd, Tb, Yb) [2,11]. The compounds R_3TiSb_5 crystallize with a hexagonal structure that is an antitype of the structure type Hf_5CuSn_3 [12], and the series $R_2Ti_7Sb_{12}$ and $R_2Ti_{11}Sb_{14}$ possess their own, partially disordered structure types ($La_2Ti_7Sb_{12}$ and $Sm_2Ti_{11}Sb_{14}$, respectively) [2,5,11]. For both structure types the inherent structural disorder is expressed as splitting of some antimony sites. $R_2Ti_{11}Sb_{14}$ also exhibits partial occupancy of one titanium site, and statistical mixing of titanium and antimony atoms, as revealed by single-crystal X-ray diffraction investigations of $Tb_2Ti_{11}Sb_{14}$ and $Yb_2Ti_{11}Sb_{14}$ that led to the compositions $Tb_2Ti_{10.41}Sb_{14.59}$ and $Yb_2Ti_{10.58}Sb_{14.42}$, respectively [11]. A compound of equiatomic composition GdTiSb with tetragonal CeFeSi-type (PbClF type) structure was reported in [13]. Magnetic and electrical transport properties were measured for the R_3TiSb_5 compounds [10], and for the $R_2Ti_{11}Sb_{14}$ compounds (*R* = Tb, Yb) electrical resistivity measurements on single crystals were performed, confirming the metallic behavior of these ternary antimonides [11]. Magnetic and transport properties were also investigated for GdTiSb [13]. Crystallographic data for ternary compounds reported in *R*–Ti–Sb systems are summarized in Table 2.

The present work reports an investigation of the phase equilibria in the Ce–Ti–Sb and Gd–Ti–Sb ternary systems at 600°C in the whole concentration range and the crystal structures of two ternary compounds, $Ce_2Ti_7Sb_{12}$ and $Gd_2Ti_{11}Sb_{14}$, determined by X-ray powder diffraction.

Experimental

0.5-gram alloys (29 alloys for the Ce–Ti–Sb system and 22 alloys for the Gd–Ti–Sb system) were prepared in an arc furnace (water-cooled copper hearth, tungsten electrode, argon atmosphere) from bulk metals with the following purities: Ce ≥ 99.9%, Gd ≥ 99.9%, Ti ≥ 99.99%, Sb ≥ 99.99%. The argon was additionally purified during the synthesis by a molten Ti getter. To ensure homogeneity the samples were melted twice. After the synthesis the samples were annealed in quartz ampoules under vacuum for one month at 600°C. Finally, the ampoules with the alloys were quenched into cold water. The weight loss did not exceed 2% of the initial mass. The number of alloys prepared for the investigation of the Ce–Ti–Sb system included a few binary alloys of the Ti–Sb system.

Phase analysis was carried out using X-ray powder diffraction data collected at room temperature on a diffractometer DRON-2.0M (Fe *Kα* radiation, λ = 1.93801 Å, angular range 30° ≤ 2θ ≤ 90°, step 0.05°). The experimental patterns were compared with simulated patterns of the metals and known

binary compounds [2], using the program STOE WinXPOW [31], and the cell parameters of the identified phases were refined using the UnitCell program [32]. The crystal structures of the ternary compounds $Ce_2Ti_7Sb_{12}$ and $Gd_2Ti_{11}Sb_{14}$ were refined on X-ray powder diffraction data collected on a powder diffractometer STOE Stadi P (Cu $K\alpha_1$ radiation, λ = 1.54056 Å, linear detector, $6° \le 2\theta \le 110°$, step 0.015°). The profile and structural parameters were refined by the Rietveld method using the FullProf Suite program package [33].

Energy-dispersive X-ray spectroscopy (EDX analysis) was carried out for particular samples on a scanning electron microscope REMMA-102-02. Pieces of alloys were placed into the cylindrical rings, the rings were then filled with Wood alloy; the surface was polished on the polishing circle using polishing paper and chromium(III) oxide.

Table 2 Crystallographic data for ternary compounds reported in *R*–Ti–Sb systems.

Compound	Structure type	Pearson symbol	Space group	Cell parameters, Å			Reference
				a	*b*	*c*	
La_3TiSb_5	Hf_5CuSn_3	*hP*18	*P*6$_3$/*mcm*	9.5294	-	6.2801	[9]
Ce_3TiSb_5	Hf_5CuSn_3	*hP*18	*P*6$_3$/*mcm*	9.4277	-	6.2316	[10]
Pr_3TiSb_5	Hf_5CuSn_3	*hP*18	*P*6$_3$/*mcm*	9.3835	-	6.2156	[10]
Nd_3TiSb_5	Hf_5CuSn_3	*hP*18	*P*6$_3$/*mcm*	9.3517	-	6.1976	[10]
Sm_3TiSb_5	Hf_5CuSn_3	*hP*18	*P*6$_3$/*mcm*	9.2758	-	6.1581	[10]
$La_2Ti_7Sb_{12}$	$La_2Ti_7Sb_{12}$	*oS*56-14	*Cmmm*	10.5446	20.768	4.4344	[5]
$Ce_2Ti_7Sb_{12}$	$La_2Ti_7Sb_{12}$	*oS*56-14	*Cmmm*	10.497	20.692	4.4160	[5]
$Pr_2Ti_7Sb_{12}$	$La_2Ti_7Sb_{12}$	*oS*56-14	*Cmmm*	10.474	20.689	4.3896	[5]
$Nd_2Ti_7Sb_{12}$	$La_2Ti_7Sb_{12}$	*oS*56-14	*Cmmm*	10.427	20.697	4.3812	[5]
$Sm_2Ti_{11}Sb_{14}$	$Sm_2Ti_{11}Sb_{14}$	*oP*64-10	*Pnma*	15.8865	5.7164	12.9244	[11]
$Gd_2Ti_{11}Sb_{14}$	$Sm_2Ti_{11}Sb_{14}$	*oP*64-10	*Pnma*	15.899	5.7198	12.938	[11]
$Tb_2Ti_{10.41}Sb_{14.59}$	$Sm_2Ti_{11}Sb_{14}$	*oP*64-10	*Pnma*	15.8693	5.7036	12.9309	[11]
$Yb_2Ti_{10.58}Sb_{14.42}$	$Sm_2Ti_{11}Sb_{14}$	*oP*64-10	*Pnma*	15.9529	5.7135	12.9442	[11]
GdTiSb	PbClF	*tP*6	*P*4/*nmm*	6.525	-	9.35	[13]

Results

Binary systems

During the phase analysis, the existence of the following binary phases was confirmed in the boundary binary systems at 600°C: Ce_2Sb, Ce_4Sb_3, CeSb, and $CeSb_2$ in the Ce–Sb system, Gd_5Sb_3, Gd_4Sb_3, GdSb, and Gd_2Sb_5 in the Gd–Sb system, Ti_3Sb, Ti_2Sb, Ti_5Sb_3, $Ti_{10,84}Sb_{7,73}$, TiSb, Ti_5Sb_8, and $TiSb_2$ in the Ti–Sb system. As expected, no binary phases were observed in the Ce–Ti and Gd–Ti systems. It should be noted that some of the binary phases with relatively high melting temperatures (TiSb, CeSb, and especially GdSb) were found as non-equilibrium phases in some of the samples. They are the first compounds that form from the molten mixture of components during arc-melting, are thermodynamically very stable and did not disappear even after one month annealing.

The compound Ce_5Sb_3 (structure type Mn_5Si_3) was not observed during our investigation in neither binary nor ternary samples.

The compound Ti_5Sb_8 was first found by EDX analysis as small amounts in a few ternary samples and as an admixture phase in the binary sample $Ti_{50}Sb_{50}$. Later on a sample of composition $Ti_{45}Sb_{55}$ was synthesized, in which the amount of this binary phase appeared to be significantly higher. Consequently, the formation of Ti_5Sb_8 in the Ti–Sb system was confirmed. Although its crystal structure has not yet been refined, it is believed to belong to the $Zr_{2.6}Ti_{2.4}Sb_8$ structure type. As mentioned above, this type was first described for the ternary phases (M',Ti)$_5Sb_8$ (M' = Zr, Hf, Nb, Mo) [4], and only later the binary phase in the Ti–Sb system was reported by Zhu and Kleinke [3]. We simulated the powder pattern of Ti_5Sb_8 using the atomic coordinates of the ternary $Zr_{2.6}Ti_{2.4}Sb_8$ structure type, and refined the cell parameters on the diffraction pattern of the sample $Ti_{45}Sb_{55}$. The resulting parameters: a = 6.4805(3), c = 26.426(3) Å, are slightly different from the cell parameters reported by Bie *et al.* (a = 6.492(4) Å, c = 26.514(15) Å) [5]. Some mismatch between the peaks of the theoretical and observed patterns also appeared, indicating that the actual structure may be slightly different from the structure of the ternary phase $Zr_{2.6}Ti_{2.4}Sb_8$, and further investigations are necessary. It should be noted that the EDX analysis of the samples containing this phase gave the composition as ~$Ti_{40}Sb_{60}$ in all the investigated alloys, leading to the chemical formula Ti_2Sb_3, as this phase was called in preliminary reports [34,35]. Due to the

uncertainty of up to ~5 at.% in the semiquantitative EDX analysis, the composition $Ti_{40}Sb_{60}$ (Ti_2Sb_3) cannot be readily distinguished from the composition $Ti_{38.46}Sb_{61.54}$ (Ti_5Sb_8). The compounds $Ti_{3.2}Sb_{0.8}$ and $Ti_{4.8}Sb_{3.3}$ were not observed during our investigation.

Ternary compounds

The formation of two ternary phases, namely Ce_3TiSb_5 (structure type Hf_5CuSn_3) and $Ce_2Ti_7Sb_{12}$ ($La_2Ti_7Sb_{12}$), in the Ce–Ti–Sb system, and one ternary phase, $Gd_2Ti_{11}Sb_{14}$ (ST $Sm_2Ti_{11}Sb_{14}$), in the Gd–Ti–Sb system, was confirmed. No other ternary phases were found in the systems at 600°C. The crystal structure of the Ce_3TiSb_5 compound was refined on X-ray single crystal data by Moore *et al*. [10], however no complete structure investigations were known for the $Ce_2Ti_7Sb_{12}$ and $Gd_2Ti_{11}Sb_{14}$ compounds, so we decided to refine these structures on X-ray powder diffraction data. The results of the refinements are given below.

To summerize the phase analysis of the samples in the Ce–Ti–Sb and Gd–Ti–Sb systems, Table 3 lists the binary and ternary phases identified at 600°C with refined cell parameters. For some of the binary compounds the parameters were refined on binary samples, and for others on ternary samples having the relevant binary phase as major component. The unit cell parameters of the Ce_3TiSb_5 compound were determined during the Rietveld refinement of the sample having a composition corresponding to the $Ce_2Ti_7Sb_{12}$ phase, which contained the Ce_3TiSb_5 phase as an admixture. The cell parameters of $TiSb_2$ were obtained from the Rietveld refinement of a sample containing a ternary phase as major component.

Table 3 Unit cell parameters of the compounds in the Ce–Ti–Sb and Gd–Ti–Sb systems observed in this work.

Compound	Sample	Structure type, Pearson symbol, space group	*a*, Å	*b*, Å	*c*, Å
$Ce_2Ti_7Sb_{12}$	$Ce_{9,53}Ti_{33,33}Sb_{57,14}$	$La_2Ti_7Sb_{12}$, *oS*56-14, *Cmmm*	10.4968(8)	20.7444(17)	4.4167(4)
Ce_3TiSb_5	$Ce_{9,53}Ti_{33,33}Sb_{57,14}$	Hf_5CuSn_3, *hP*18, *P*6$_3$/*mcm*	9.4269(8)	-	6.2423(6)
Ce_2Sb	$Ce_{62,5}Ti_{10}Sb_{27,5}$	La_2Sb, *tI*12, *I*4/*mmm*	4.5289(3)	-	17.8607(14)
Ce_4Sb_3	$Ce_{50}Ti_{10}Sb_{40}$	Th_3P_4, *cI*28, *I*-43*d*	9.5237(3)	-	-
CeSb	$Ce_{22,22}Ti_{33,33}Sb_{44,45}$	NaCl, *cF*8, *Fm*-3*m*	6.4148(2)	-	-
$CeSb_2$	$Ce_{33,33}Sb_{66,67}$	$SmSb_2$, *oS*24, *Cmce*	6.2687(6)	6.1448(6)	18.2691(10)
$Gd_2Ti_{11}Sb_{14}$	$Gd_{7,41}Ti_{40,74}Sb_{51,85}$	$Sm_2Ti_{11}Sb_{14}$, *oP*64-10, *Pnma*	15.9113(13)	5.7158(3)	12.9385(9)
Gd_5Sb_3	$Gd_{57,5}Ti_{10}Sb_{32,5}$	Mn_5Si_3, *hP*16, *P*6$_3$/*mcm*	9.0219(3)	-	6.3204(3)
Gd_4Sb_3	$Gd_{50}Ti_{10}Sb_{40}$	Th_3P_4, *cI*28, *I*-43*d*	9.2240(3)	-	-
GdSb	$Gd_{33,33}Ti_{11,11}Sb_{55,55}$	NaCl, *cF*8, *Fm*-3*m*	6.2144(2)	-	-
Gd_2Sb_5	$Gd_{25}Sb_{75}$	Dy_2Sb_5, *mP*28, *P*2$_1$/*m*	13.1668(7)	4.18428(3) β = 102.435(4)°	14.7366(10)
Ti_3Sb	$Ti_{75}Sb_{25}$	Cr_3Si, *cP*8, *Pm*-3*n*	5.2180(2)	-	-
Ti_2Sb	$Ti_{66.67}Sb_{33,33}$	Ti_2Bi, *tI*12, *I*4/*mmm*	3.9483(3)	-	14.5893(7)
Ti_5Sb_3	$Gd_{9,09}Ti_{54,54}Sb_{36,36}$	Yb_5Sb_3, *oP*32, *Pnma*	10.2133(16)	8.3423(15)	7.1659(4)
$Ti_{10,84}Sb_{7,73}$	$Ti_{58,37}Sb_{41,63}$	$Cr_{11}Ge_8$, *oP*76, *Pnma*	14.6577(6)	5.5490(2)	17.6509(9)
TiSb	$Ti_{50}Sb_{50}$	NiAs, *hP*4, *P*6$_3$/*mmc*	4.0139(2)	-	6.2573(3)
Ti_5Sb_8	$Ti_{40}Sb_{60}$	$Zr_{2.6}Ti_{2.4}Sb_8$, *tI*52, *I*4$_1$22	6.4805(3)	-	26.426(3)
$TiSb_2$	$Ce_{9,53}Ti_{33,33}Sb_{57,14}$	$CuAl_2$, *tI*12, *I*4/*mcm*	6.6539(5)	-	5.8109(4)

EDX analysis of particular samples

The microstructures of several samples were studied by energy-dispersive X-ray spectroscopy. One of the most important results appeared to be the presence of the Ti_5Sb_8 phase in the samples $Ti_{50}Sb_{50}$ and $Gd_{7.41}Ti_{40.74}Sb_{51.85}$ as a small admixture, proving that this compound really exists in the binary Ti–Sb system and the ternary systems. After the confirmation of the existence of the compound by EDX, a sample of composition $Ti_{45}Sb_{55}$ was synthesized, which contained a significant amount of the Ti_5Sb_8 phase.

The solubility of the third component in some of the binary phases and their homogeneity ranges in the binary systems were also investigated by EDX analysis. However, taking into account the uncertainty of up to ~5 at.% in semiquantitative EDX analysis, solubilities of the third component in the binary phases, deviations from the ideal compositions of the compounds, and homogeneity ranges smaller than 5 at.%, were considered as negligible. The only significant solubilities were observed for Sb in Ti (~9.8 at.%) and Ti in GdSb (~5 at.%) (substitution of Ti for Gd in the structure). The results of the EDX analysis are summarized in Table 4, while Fig. 1 shows the microstructures of three samples.

Table 4 Results of the EDX analysis of selected samples in the Ce–Ti–Sb and Gd–Ti–Sb systems.

Sample	Phase	Composition from EDX analysis
$Ce_{9,53}Ti_{33,33}Sb_{57,14}$	$Ce_2Ti_7Sb_{12}$ Ce_3TiSb_5	$Ce_{7.5}Ti_{40.1}Sb_{52.4}$ $Ce_{30.2}Ti_{12.1}Sb_{57.7}$
$Ce_{22.22}Ti_{33.33}Sb_{44.45}$	TiSb CeSb Ti_5Sb_3	$Ce_{3.4}Ti_{50.3}Sb_{46.3}$ $Ce_{45.9}Ti_{1.1}Sb_{53.0}$ $Ti_{61.9}Sb_{38.1}$
$Ce_{33.33}Ti_{33.33}Sb_{33.34}$	(Ti) Ce_4Sb_3	$Ti_{90.2}Sb_{9.8}$ $Ce_{52.3}Ti_{2.7}Sb_{45.0}$
$Ce_{40}Ti_{40}Sb_{20}$	(Ti) Ce_2Sb	$Ce_{1.8}Ti_{98.2}$ $Ce_{63.4}Ti_{0.3}Sb_{36.3}$
$Gd_{7,41}Ti_{40,74}Sb_{51,85}$	$Gd_2Ti_{11}Sb_{14}$ GdSb Ti_5Sb_8 TiSb	$Gd_{4.0}Ti_{48.4}Sb_{47.6}$ $Gd_{42.5}Ti_{5.0}Sb_{52.5}$ $Gd_{1.5}Ti_{38.3}Sb_{60.2}$ $Gd_{0.2}Ti_{50.2}Sb_{49.6}$
$Gd_{57.5}Ti_{10}Sb_{32.5}$	(Ti) Gd_4Sb_3	$Gd_{3.2}Ti_{96.4}Sb_{0.4}$ $Gd_{58.3}Ti_{1.5}Sb_{40.2}$
$Gd_{40}Ti_{40}Sb_{20}$	(Ti) Gd_4Sb_3	$Gd_{3.3}Ti_{96.3}Sb_{0.4}$ $Gd_{57.3}Ti_{1.8}Sb_{40.9}$
$Ti_{50}Sb_{50}$	TiSb Ti_5Sb_8	$Ti_{49.8}Sb_{50.2}$ $Ti_{40.0}Sb_{60.0}$
$Ti_{58.37}Sb_{41.63}$	$Ti_{10.84}Sb_{7.73}$ Ti_5Sb_3	$Ti_{58.2}Sb_{41.8}$ $Ti_{62.3}Sb_{37.7}$
$Ti_{71.43}Sb_{28.57}$	Ti_2Sb Ti_3Sb	$Ti_{66.0}Sb_{34.0}$ $Ti_{75.3}Sb_{24.7}$
$Ti_{80}Sb_{20}$	Ti_3Sb	$Ti_{77.4}Sb_{22.6}$

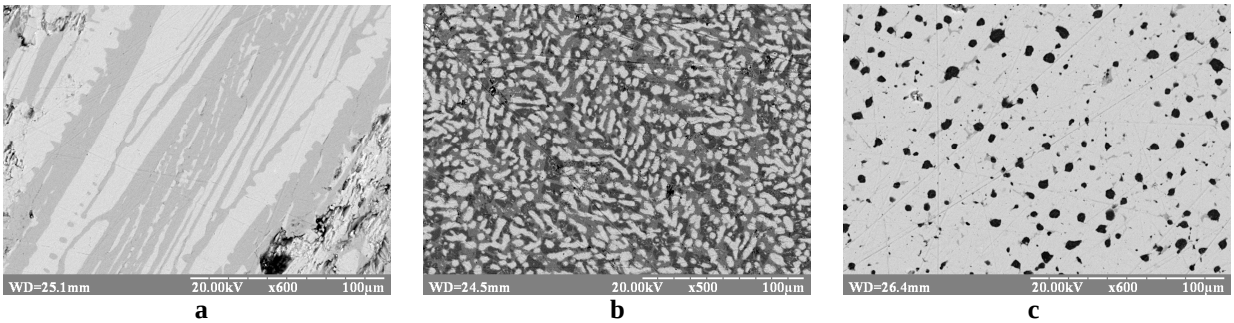

a **b** **c**

Fig. 1 Microstructures of some samples of the Ce–Ti–Sb and Gd–Ti–Sb systems: a) $Ti_{71.43}Sb_{28.57}$ (light phase – Ti_2Sb, grey phase – Ti_3Sb); b) $Ce_{22.22}Ti_{33.33}Sb_{44.45}$ (light phase – CeSb, grey phase – TiSb, dark grey phase – Ti_5Sb_3); c) $Gd_{57.5}Ti_{10}Sb_{32.5}$ (light phase – Gd_4Sb_3, dark phase – (Ti))

Isothermal sections of the phase diagrams of the Ce–Ti–Sb and Gd–Ti–Sb systems at 600°C

The isothermal section of the phase diagram of the ternary Ce–Ti–Sb system at 600°C is shown in Fig. 2. It consists of 16 single-phase, 31 two-phase, and 16 three-phase fields. The highest number of equilibria (8) is formed with the binary CeSb phase. The section of this system at 600°C is very similar to the isothermal section of the phase diagram of the La–Ti–Sb system at 800°C constructed by Bie *et al.* [5], a significant difference being, however, the presence of the Ti_5Sb_8 compound in the section constructed here.

The isothermal section at 600°C of the phase diagram of the ternary Gd–Ti–Sb system is shown in Fig. 3. It consists of 15 single-phase, 28 two-phase, and 14 three-phase fields. The highest number of equilibria (10) is formed with the binary GdSb phase.

In agreement with the results of the EDX analysis, the diagrams show a solubility of antimony in titanium of up to ~9.8 at.%, and of titanium in the GdSb compound of up to ~5 at.%.

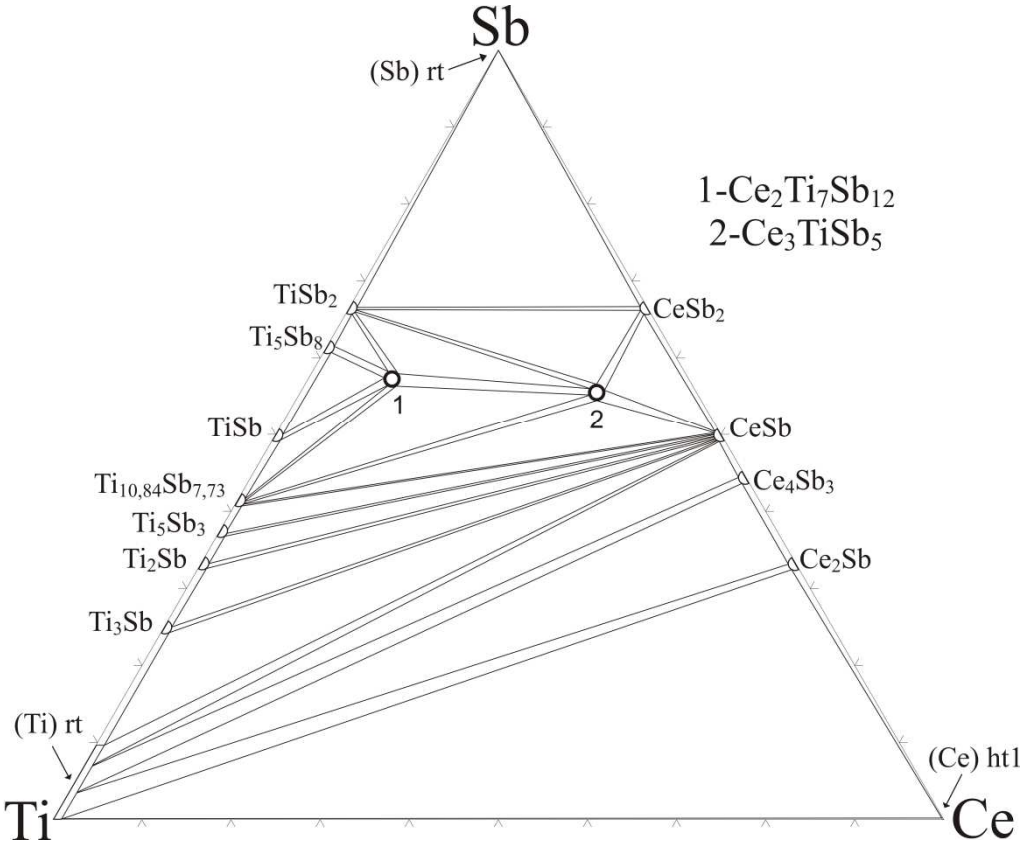

Fig. 2 Isothermal section of the phase diagram of the ternary Ce–Ti–Sb system at 600°C.

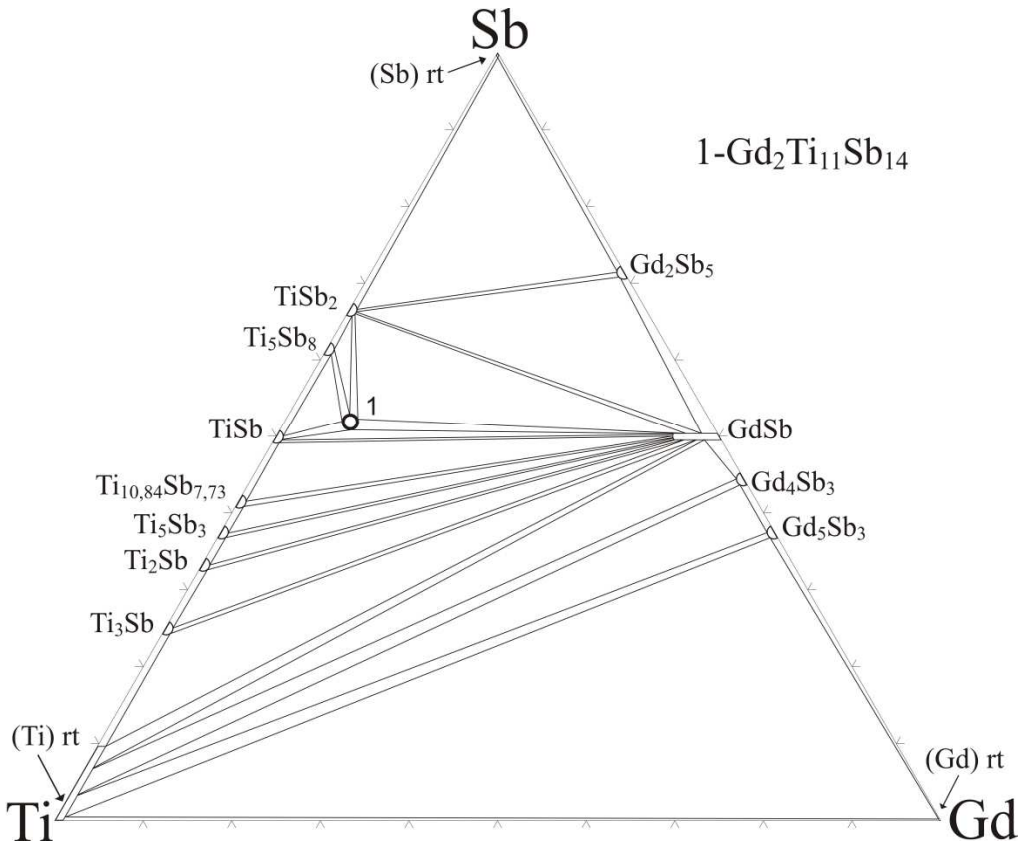

Fig. 3 Isothermal section of the phase diagram of the ternary Gd–Ti–Sb system at 600°C.

Crystal structure of the $Ce_2Ti_7Sb_{12}$ compound

The crystal structure of the ternary phase $Ce_2Ti_7Sb_{12}$ was known to belong to the $La_2Ti_7Sb_{12}$ structure type; however, no structure refinement had been performed. Fig. 4 shows the diffraction pattern of the sample of nominal composition $Ce_{9,53}Ti_{33,33}Sb_{57,14}$ and the results of the Rietveld refinement are presented in Table 5. The sample contains three phases: $Ce_2Ti_7Sb_{12}$, $TiSb_2$, and Ce_3TiSb_5. For the $Ce_2Ti_7Sb_{12}$ compound the atomic coordinates and $B_{iso/ov}$ were refined. Table 6 lists the final atomic coordinates and site occupancies of the structure, and Table 7 selected interatomic distances, coordination numbers and coordination polyhedra.

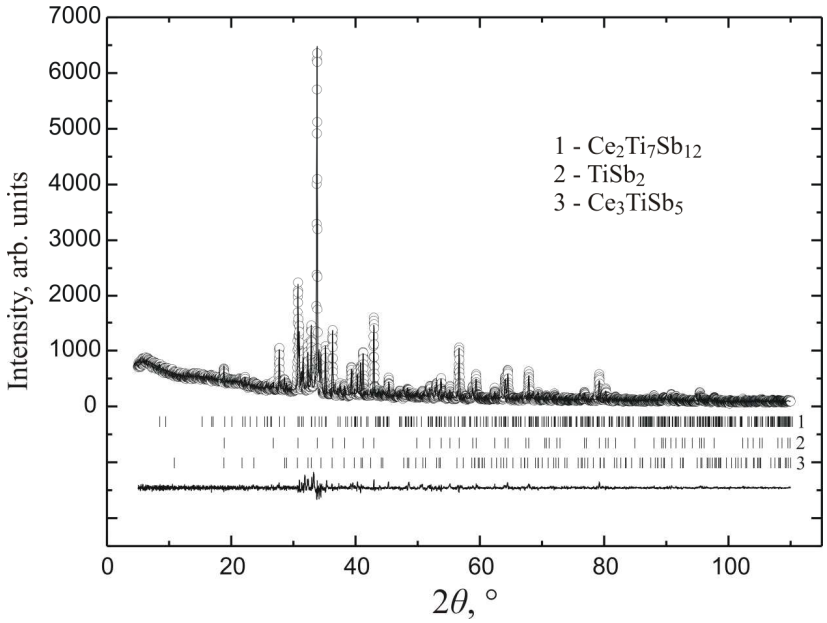

Fig. 4 Experimental (circles), calculated (solid line) and difference (bottom) X-ray diffraction patterns of the sample $Ce_{9,53}Ti_{33,33}Sb_{57,14}$. Vertical ticks show the positions of the reflections of the individual phases.

Table 5 Experimental details and crystallographic parameters of the individual phases in the sample $Ce_{9,53}Ti_{33,33}Sb_{57,14}$.

Compound	$Ce_2Ti_7Sb_{12}$	$TiSb_2$	Ce_3TiSb_5
Content, mass%	44.5(7)	46.6(4)	8.92(14)
Structure type	$La_2Ti_7Sb_{12}$	$CuAl_2$	Hf_5CuSn_3
Pearson symbol	*oS*56-14	*tI*12	*hP*18
Space group	*Cmmm* (#65)	*I*4/*mcm* (#140)	$P6_3/mcm$ (#193)
Cell parameters: *a*, Å	10.4968(8)	6.6539(5)	9.4269(8)
b, Å	20.7444(17)	-	-
c, Å	4.4167(4)	5.8109(4)	6.2423(6)
Cell volume *V*, Å^3	961.73(13)	257.28(3)	480.42(7)
Formula units per unit cell *Z*	2	4	2
Density D_x, g/cm^3	7.171	7.523	7.445
Preferred orientation: value [direction]	0.929(6) [001]	-	-
FWHM parameters: *U*		-0.014(7)	
V		0.049(7)	
W		0.0070(16)	
Shape parameter η		0.448(12)	
Asymmetry parameters		0.162(8), 0.007(19)	
Reliability factors: R_B	0.117	0.0463	0.155
R_F	0.128	0.0639	0.119
R_p		0.0595	
R_{wp}		0.0816	
R_{exp}		0.0607	
χ^2		1.82	

Table 6 Atomic coordinates and site occupancies for the $Ce_2Ti_7Sb_{12}$ compound ($B_{iso/ov}$ = 1.13(9) Å^2).

Site	Wyckoff position	*x*	*y*	*z*	Occupancy
Ce	4*i*	0	0.3914(4)	0	1
Ti1	8*p*	0.1488(16)	0.1183(9)	0	1
Ti2	4*e*	¼	¼	0	1
Ti3	2*a*	0	0	0	1
Sb1	8*q*	0.2922(6)	0.1653(4)	½	1
Sb2	8*o*	0.2607(11)	0	0.130(3)	0.5
Sb3	8*n*	0	0.2306(7)	0.149(3)	0.5
Sb4	4*j*	0	0.0780(6)	½	1
Sb5	4*j*	0	0.2211(19)	½	0.25
Sb6	4*h*	0.182(4)	0	½	0.25
Sb7	2*c*	½	0	½	1

Table 7 Selected interatomic distances (δ), coordination numbers (CN) and polyhedra in the structure of the $Ce_2Ti_7Sb_{12}$ compound.

Atoms	δ, Å	CN	Polyhedron
Ce - 2Sb7 - 4Sb1 - Sb3 - 2Sb2	3.152(6) 3.328(6) 3.406(15) 3.425(11)	9	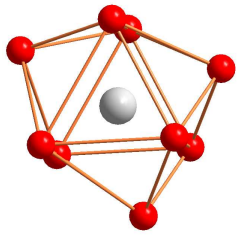 $CeSb_9$
Ti1 - Sb2 - 2Sb4 - 2Sb1 - Sb3	2.774(19) 2.830(12) 2.841(12) 2.88(2)	6	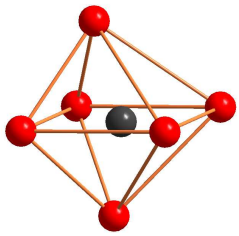 $Ti1Sb_6$
Ti2 - 2Sb3 - 4Sb1	2.736(4) 2.855(4)	6	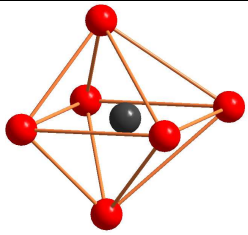 $Ti2Sb_6$
Ti3 - 4Sb4 - 2Sb2	2.738(6) 2.786(12)	6	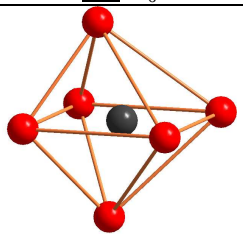 $Ti3Sb_6$

Continuation of **Table 7**

Sb1 - 2Ti1 - 2Ti2 - Sb5 - Sb5 - 2Ce	2.841(12) 2.855(4) 3.22(3) 3.266(15) 3.328(6)	8	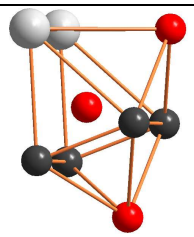 Sb1Ce$_2$Ti$_4$Sb$_2$
Sb2 - 2Ti1 - Ti3 - Sb7 - 2Sb2/Sb6	2.774(19) 2.786(12) 3.009(13) 3.286(19)/2.867(17)	6	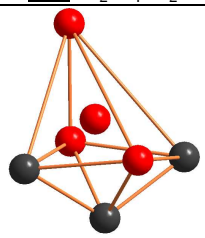 Sb2Ti$_3$Sb$_3$
Sb3 - 2Ti2 - 2Ti1 - 2Sb3/Sb5 - Ce	2.736(4) 2.88(2) 3.101(19)/2.874(14) 3.406(15)	7	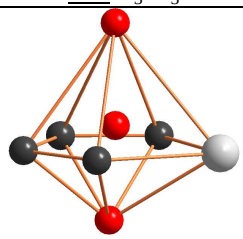 Sb3CeTi$_4$Sb$_2$
Sb4 -2Sb6 - 2Ti3 - 4Ti1 - Sb5	2.58(4) 2.738(7) 2.830(12) 2.96(4)	9	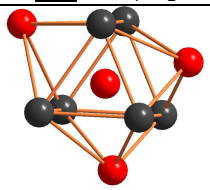 Sb4Ti$_6$Sb$_3$
Sb5 - 2Sb3 - Sb4 - 2Sb1 - 2Sb1	2.874(14) 2.96(4) 3.22(3) 3.266(15)	7	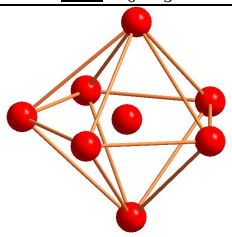 Sb5Sb$_7$
Sb6 - 2Sb4 - 2Sb2 - 2Ti3 - 4Ti1	2.58(4) 2.867(17) 2.98(3) 3.330(15)	10	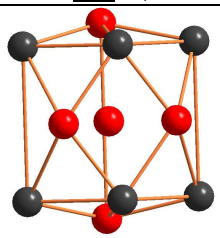 Sb6Ti$_6$Sb$_4$
Sb7 - 4Sb2/2Sb6 - 4Ce	3.009(13)/3.24(5) 3.152(6)	8	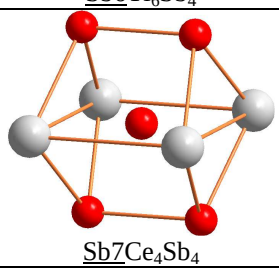 Sb7Ce$_4$Sb$_4$

The crystal structure of the $Ce_2Ti_7Sb_{12}$ compound is shown in Fig.5. It is relatively complex and partly disordered. Since it was not possible to obtain single crystals for a more accurate determination of the crystal structure, the atomic parameters in the $La_2Ti_7Sb_{12}$ structure type were used as starting positions and the occupancies of the four partly occupied antimony sites were fixed to the values given in [5].

The disorder in the structure corresponds to the partial occupancy of four of the antimony sites: Sb2 and Sb3 both have an occupancy of 0.5, Sb5 and Sb6 an occupancy of 0.25. These numbers are imposed by the model since in the case of full occupancy impossibly short Sb-Sb interatomic distances would appear. The partially occupied sites are located close to one another forming the following pairs: Sb2 (occupancy 0.5) is close to Sb6 (0.25), and Sb3 (0.5) close to Sb5 (0.25). Bie *et al.* [5] proposed a possible model for local ordering of these sites within the chains of edge-sharing Ti1-centered octahedra that extend along the *c*-direction in the structure. All the titanium atoms center slightly distorted tetragonal bipyramids (octahedra), whereas the coordination polyhedra of the rare-earth metal atoms are tricapped trigonal prisms. Exclusively antimony atoms form the coordination polyhedra of both the titanium and rare-earth metal atoms. Various types of polyhedron surround the different antimony sites. These are quite difficult to derive because it is necessary to take into account the partial occupancies of some of the Sb sites. In Table 7 idealized polyhedra are proposed for the Sb atoms, but in some cases, due to the presence of Sb atoms from the partially occupied sites Sb5 and Sb6 (occupancy 0.25), several polyhedra are possible. For example, the coordination number of the site Sb7 can vary from 6 to 8 since, in addition to the four Ce atoms, it can be coordinated by four Sb2 atoms or two Sb6 atoms (in the case of presence of Sb6 atoms the polyhedron will be a bipyramid). Coordination by 2 Sb2 atoms on one side and one Sb6 atom on the other side is also possible, leading to a total CN = 7. As stated above, full occupancy of the partially occupied sites would lead to the appearance of several impossibly short interatomic distances within the chains of the antimony atoms along [001]: Sb2-Sb2 (1.131(19) Å), Sb2-Sb6 (1.80(3) Å), Sb3-Sb3 (1.316(19) Å), Sb3-Sb5 (1.563(15) Å). The complex three-dimensional framework formed by the octahedra around the Ti atoms in the structure of the $La_2Ti_7Sb_{12}$-type compounds is shown in Fig. 5.

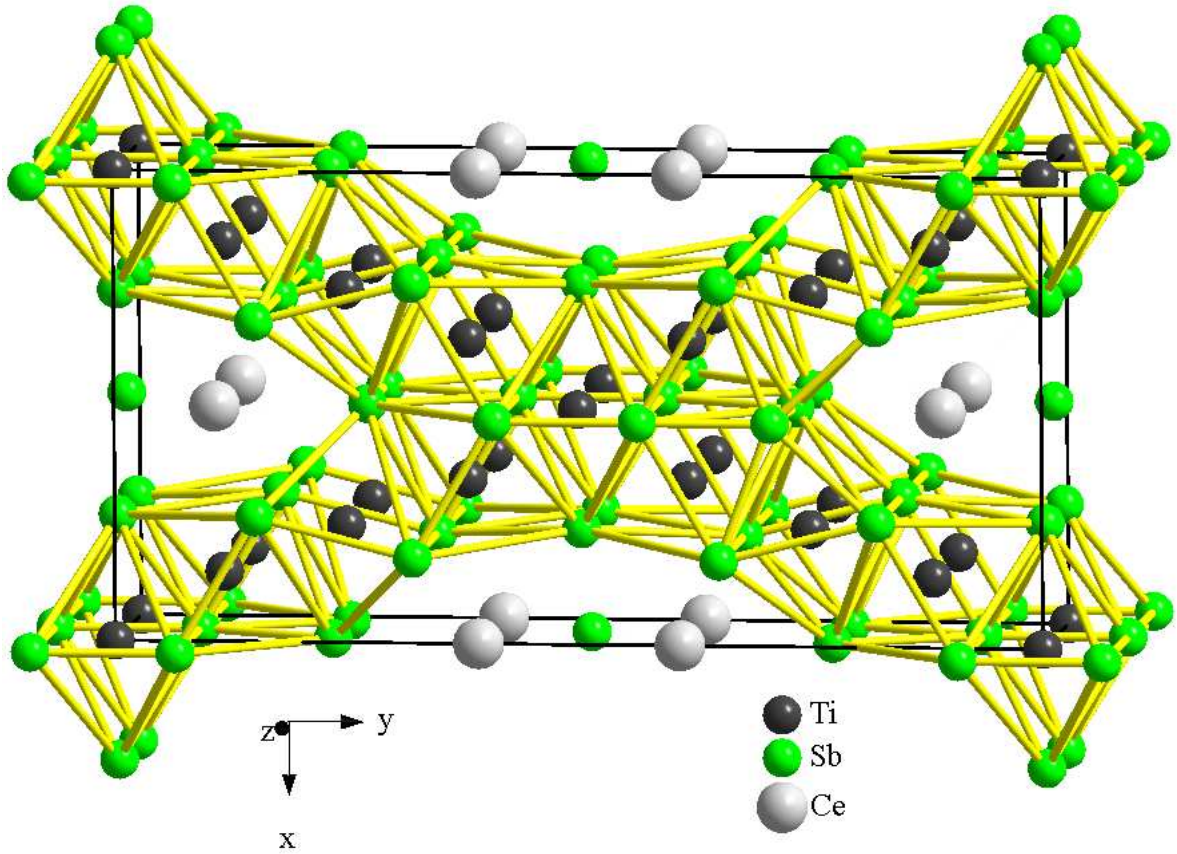

Fig. 5 Projection of the crystal structure of the $Ce_2Ti_7Sb_{12}$ compound onto the *XY* plane. The three-dimensional framework of distorted octahedra around the Ti atoms is shown (for the split sites Sb2 and Sb3, and the partially occupied sites Sb5 and Sb6, only one member of each set is shown).

Crystal structure of the $Gd_2Ti_{11}Sb_{14}$ compound

The crystal structure of the ternary phase $Gd_2Ti_{11}Sb_{14}$ belongs to the $Sm_2Ti_{11}Sb_{14}$ structure type. The results of the Rietveld refinement of the sample with nominal composition $Gd_{7.41}Ti_{40.74}Sb_{51.85}$ are given in Table 8 and Fig. 6 shows a comparison of the experimental and simulated diffraction patterns. The sample contains four phases: $Gd_2Ti_{11}Sb_{14}$, $TiSb_2$, TiSb, and GdSb (the latter is believed to be a non-equilibrium admixture). For the $Gd_2Ti_{11}Sb_{14}$ compound the atomic coordinates and $B_{iso/ov}$ were refined; the atomic coordinates and site occupancies are listed in Table 9, and selected interatomic distances, coordination numbers and polyhedra are given in Table 10. The crystal structure of the $Gd_2Ti_{11}Sb_{14}$ compound is shown in Fig. 7.

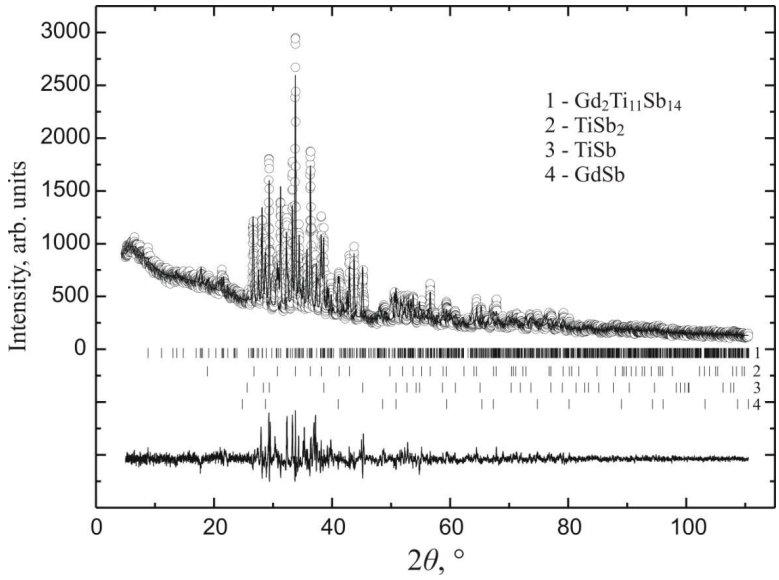

Fig. 6 Experimental (circles), calculated (solid line) and difference (below) X-ray powder diffraction patterns of the sample $Gd_{7.41}Ti_{40.74}Sb_{51.85}$. Vertical ticks show the positions of the reflections from the individual phases.

Table 8 Experimental details and crystallographic parameters for the individual phases in the sample $Gd_{7.41}Ti_{40.74}Sb_{51.85}$.

Compound	$Gd_2Ti_{11}Sb_{14}$	$TiSb_2$	TiSb	GdSb
Content, mass%	70.8(12)	15.8(3)	10.4(2)	2.97(10)
Structure type	$Sm_2Ti_{11}Sb_{14}$	$CuAl_2$	NiAs	NaCl
Pearson symbol	*oP*64-10	*tI*12	*hP*4	*cF*8
Space group	*Pnma* (#62)	*I*4/*mcm* (#140)	$P6_3/mmc$ (#194)	*Fm*-3*m* (#225)
Cell parameters: *a*, Å	15.9113(13)	6.6521(8)	4.0053(5)	6.2176(6)
b, Å	5.7158(3)	-	-	-
c, Å	12.9385(9)	5.8096(8)	6.2857(13)	-
Cell volume *V*, Å^3	1176.69(14)	257.68(5)	87.56(2)	240.36(5)
Formula units per unit cell *Z*	2	4	2	4
Density D_x, g/cm^3	7.185	7.511	6.434	7.710
Preferred orientation: value [direction]	0.932(6) [010]	-	-	-
FWHM parameters: *U*	0.49(6)			
V	-0.34(5)			
W	0.088(8)			
Shape parameter η	0.56(2)			
Asymmetry parameters	0.082(11), -0.019(4)			
Reliability factors: R_B	0.170	0.0799	0.154	0.0830
R_F	0.109	0.0716	0.0994	0.0689
R_p	0.0682			
R_{wp}	0.0946			
R_{exp}	0.0509			
χ^2	3.46			

Table 9 Atomic coordinates and site occupancies for $Gd_2Ti_{11}Sb_{14}$ compound ($B_{iso/ov}$ = 1.10(10) Å^2).

Site	Wyckoff position	*x*	*y*	*z*	Occupancy
Gd	4*c*	0.3465(9)	¼	0.0527(11)	1
Ti1	8*d*	0.3888(15)	-0.004(5)	0.4793(18)	1
Ti2	4*c*	0.038(5)	¼	0.179(6)	0.5
Ti3	4*c*	0.068(3)	¼	0.725(3)	1
Ti4	4*c*	0.203(3)	¼	0.370(4)	1
Ti5	4*c*	0.361(3)	¼	0.722(4)	1
Sb1	8*d*	0.0315(7)	0.507(3)	0.3772(8)	1
Sb2	4*c*	0.1549(19)	¼	0.173(3)	0.5
Sb3	4*c*	0.2018(17)	¼	0.144(3)	0.5
Sb4	4*c*	0.2175(10)	¼	0.5888(12)	1
Sb5	4*c*	0.2551(9)	¼	0.8485(12)	1
Sb6	4*c*	0.350(3)	¼	0.290(3)	0.5
Sb7	4*c*	0.372(3)	¼	0.340(3)	0.5
Sb8	4*c*	0.507(2)	¼	0.5614(10)	1

Table 10 Selected interatomic distances (δ), coordination numbers (CN) and polyhedra in the structure of the $Gd_2Ti_{11}Sb_{14}$ compound.

Atoms	δ, Å	CN	Polyhedron
Gd - Sb5 - 2Sb4 - Sb6/Sb7 - 2Sb1 - 2Sb1 - Sb2/Sb3	3.02(2) 3.070(8) 3.07(4)/3.74(3) 3.295(17) 3.413(16) 3.42(4)/2.59(4)	9	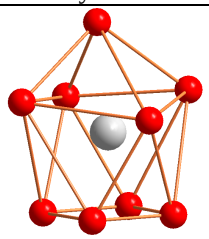 GdSb$_9$
Ti1 - Sb8 - Sb8 - Ti1 - Ti1 - 2Sb6/Sb7 - Sb2/Sb3 - Ti2	2.24(4) 2.60(4) 2.81(4) 2.90(4) 2.91(4)/2.33(4) 2.96(4)/2.93(4) 3.17(3)	8	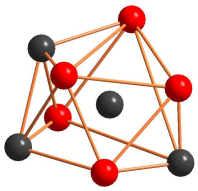 Ti1Ti$_3$Sb$_5$
Ti2 - Sb3 - 2Sb1 - Sb6 - 2Sb8 - Sb8	2.65(3) 2.951(10) 3.01(4) 3.154(12) 3.317(8)	7	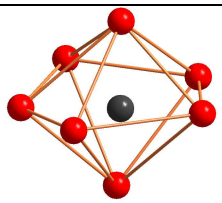 Ti2Sb$_7$
Ti3 - 2Sb1 - Sb8 - Sb4 - 2Sb6/Sb7 - Sb5	2.49(3) 2.93(4) 2.96(4) 3.25(3)/3.36(3) 3.38(4)	7	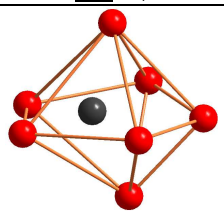 Ti3Sb$_7$

Continuation of **Table 10**

Ti4 - Sb6/Sb7 - Sb2/Sb3 - Sb4 - 2Sb5 - 2Sb1	2.56(5)/2.72(5) 2.66(5)/2.92(6) 2.84(4) 2.948(9) 3.10(3)	7	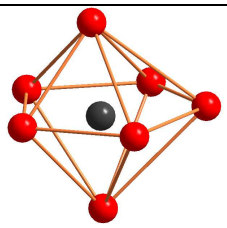 Ti4Sb$_7$
Ti5 - Sb5 - Sb4 - 2Sb2/Sb3 - 2Sb1 - Sb8	2.35(4) 2.86(4) 2.938(11)/3.19(3) 2.98(4) 3.12(5)	7	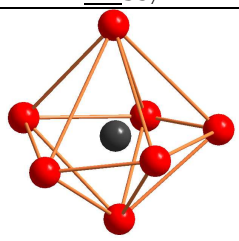 Ti5Sb$_7$
Sb1 - Ti3 - Sb1 - Ti2 - Sb1 - Ti5 - Ti4 - Gd - Sb1 - Gd	2.49(4) 2.778(17) 2.938(17) 2.951(10) 2.98(4) 3.10(4) 3.295(17) 3.333(14) 3.413(16)	9	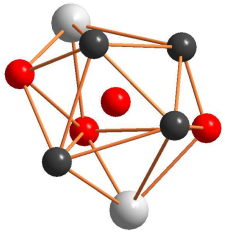 Sb1Gd$_2$Ti$_4$Sb$_3$
Sb2 - Ti4 - 2Ti5 - 2Ti1 - Gd	2.66(5) 2.938(11) 2.96(4) 3.42(4)	6	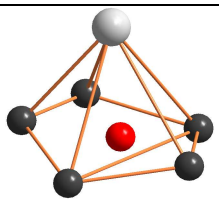 Sb2GdTi$_6$
Sb3 - Gd - Ti2 - Ti4 - 2Ti1 - Sb6 - 2Ti5 - 2Sb4	2.59(4) 2.65(3) 2.92(6) 2.93(4) 3.02(5) 3.19(3) 3.214(16)	10	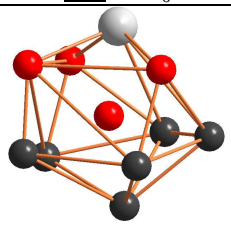 Sb3GdTi$_6$Sb$_3$
Sb4 - Ti4 - Ti5 - Ti3 - 2Gd - 2Ti1 - 2Sb2/Sb3	2.84(5) 2.86(4) 2.96(4) 3.070(8) 3.40(3) 3.67(3)/3.214(16)	9	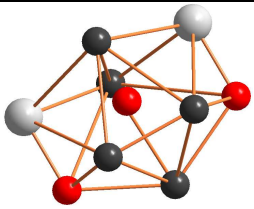 Sb4Gd$_2$Ti$_5$Sb$_2$
Sb5 - Ti5 - 2Ti4 - Gd - 2Ti1 - Ti3	2.35(4) 2.948(9) 3.02(3) 3.17(3) 3.38(4)	7	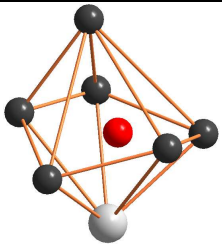 Sb5GdTi$_6$

Continuation of **Table 10**

Sb6 - Ti4 - 2Ti1 - Ti2 - Gd - 2Ti3 - Sb2/Sb3	2.56(5) 2.91(5) 3.01(4) 3.07(5) 3.25(3) 3.45(5)/3.02(5)	8	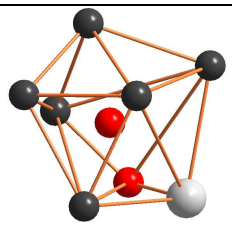 Sb6GdTi$_6$Sb
Sb7 - 2Ti1 - Ti2 - Ti4 - 2Ti3	2.33(4) 2.65(4) 2.72(5) 3.36(3)	6	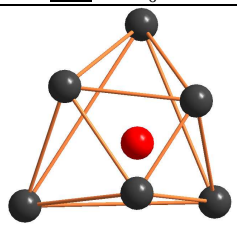 Sb7Ti$_6$
Sb8 - 2Ti1 - 2Ti1 - Ti3 - Ti5	2.24(4) 2.60(4) 2.93(5) 3.12(5)	6	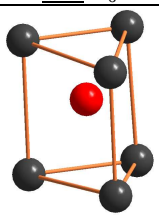 Sb8Ti$_6$

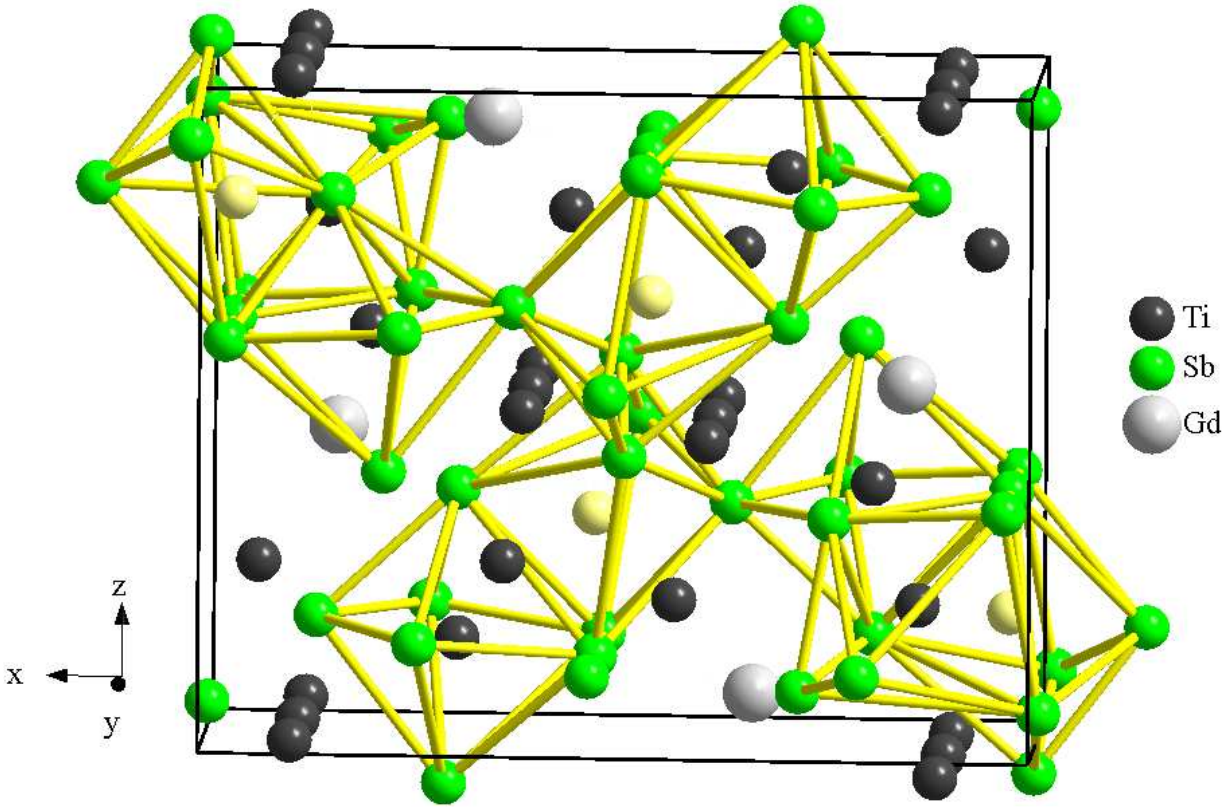

Fig. 7 Crystal structure of the $Gd_2Ti_{11}Sb_{14}$ compound viewed along the *y* direction. The three-dimensional framework of pentagonal bipyramids centered by atoms of the sites Ti2, Ti3 and Ti4 is shown (for the split sites Sb2/Sb3 and Sb6/Sb7, only one member of each set is shown, and the partially occupied Ti2 site is shown with lighter color).

According to the investigations carried out by Bie and Mar [11], the structure of the $R_2Ti_{11}Sb_{14}$ compounds is also relatively complex and exhibits several types of structural disorder: 1) split Sb sites, 2) partial occupancy of one of the Ti sites, and 3) mixing of Ti and Sb atoms. During the refinement performed here, only the first two types of disorder were taken into consideration, because the study of mixing of Ti and Sb atoms requires high-quality data, preferably from single crystals. Since no single crystals were available, the composition was fixed to the ideal ratio of 2:11:14 in the refinement. However, the semiquantitative EDX analysis gave the composition of the ternary phase in the sample $Gd_{7.41}Ti_{40.74}Sb_{51.85}$ as ~$Gd_{4.0}Ti_{48.4}Sb_{47.6}$, indicating that the compound may have a certain homogeneity range.

As in the structure of the $R_2Ti_7Sb_{12}$ compounds, in the $R_2Ti_{11}Sb_{14}$ compounds the rare-earth metal atoms center tricapped trigonal prisms formed exclusively by Sb atoms. The titanium atoms center slightly distorted pentagonal bipyramids formed by Sb atoms, except for the Ti1 site, which has a different polyhedron. The coordination of the Ti atoms is one of the main features distinguishing the $R_2Ti_{11}Sb_{14}$ compounds from the $R_2Ti_7Sb_{12}$ ones, where the Ti atoms center tetragonal bipyramids (octahedra). A common feature of the two series of compounds is the variety of coordination polyhedra around the Sb atoms and the possibility of alternative interatomic distances and coordination numbers because of splitting and partial occupancy of some sites. Also here full occupancy of these sites would result in several impossibly short interatomic distances: Sb2-Sb3 (0.84(5) Å), Sb6-Sb7 (0.74(5) Å), Sb2-Ti2 (1.87(4) Å). Like the distorted octahedra in the structure of the $La_2Ti_7Sb_{12}$-type compounds, the pentagonal bipyramids centered by Ti atoms in the structures of the $R_2Ti_{11}Sb_{14}$ compounds form a three-dimensional framework by sharing Sb atoms.

Discussion

From the results of our investigation it can be seen that the ternary systems Ce–Ti–Sb and Gd–Ti–Sb are relatively similar regards the phase equilibria observed at 600°C. The Ce–Sb and Gd–Sb systems contain two pairs of isotypic binary compounds: CeSb and GdSb, Ce_4Sb_3 and Gd_4Sb_3. Among the binaries of these systems, the CeSb and GdSb compounds have the highest melting points (1800°C and 2130°C, respectively [1]) and form the highest number of equilibria with other phases in the ternary systems. The equilibria common to both the ternary systems are the following: CeSb-$Ti_{10.84}Sb_{7.73}$, CeSb-Ti_5Sb_3, CeSb-Ti_2Sb, CeSb-Ti_3Sb, CeSb-(Ti), Ce_4Sb_3-(Ti) in the Ce–Ti–Sb system, and the corresponding equilibria GdSb-$Ti_{10.84}Sb_{7.73}$, GdSb-Ti_5Sb_3, GdSb-Ti_2Sb, GdSb-Ti_3Sb, GdSb-(Ti), Gd_4Sb_3-(Ti) in the Gd–Ti–Sb system. The main differences in the phase diagrams are related to the existence of two ternary compounds in the Ce–Ti–Sb system at this temperature, but only one in the Gd–Ti–Sb system. This makes the phase diagram of the system with cerium more complex, with a higher number of equilibria in the isothermal section. The solid solubilities of the third component in the binary phases are small and negligible, the only exception being the solubility of about 5 at.% Ti in the GdSb compound.

The compositions of the ternary compounds formed in the systems with cerium and gadolinium differ, indicating that the electronic factor is of major importance for the formation of ternaries in the *R*–Ti–Sb systems. R_3TiSb_5 phases are known only for *R* = La-Nd and Sm, $R_2Ti_7Sb_{12}$ only for *R* = La-Nd, and $R_2Ti_{11}Sb_{14}$ for *R* = Sm, Gd, Tb, and Yb. It follows that the systems with early lanthanides are characterized by the formation of two compounds, while the formation of only one compound has been reported for *R* = Gd, Tb, and Yb. Attempts to synthesize ternary compounds isotypic with the abovementioned compounds with other late lanthanides failed [11], and no ternary compounds are known in these systems sofar. Samarium forms Sm_3TiSb_5 and $Sm_2Ti_{11}Sb_{14}$ compounds, confirming its position as boundary metal between the early and late lanthanides by forming one compound typical for the early, and one compound typical for the late lanthanides.

As mentioned in the introduction, among the ternary *R*–Ti–Sb systems isothermal sections of only two systems (La–Ti–Sb and Er–Ti–Sb) had been constructed up to now. The isothermal section at 600°C of the Ce–Ti–Sb system is nearly equal to the isothermal section at 800°C of the La–Ti–Sb system constructed by Bie *et al.* [5]. The only differences are the presence of the Ti_5Sb_8 compound at 600°C and the presence of an R_5Sb_3 compound in the La–Ti–Sb system. The isothermal section of the Er–Ti–Sb system at 800°C constructed by Bie *et al.* [5] contains no ternary compounds and only two binaries in the Er–Sb system (Er_5Sb_3 and ErSb). One may conclude that the formation of ternary compounds in the *R*–Ti–Sb systems is more favorable with the early lanthanides, probably mainly due to the electronic factor and maybe in part also to the size of the rare-earth metal atoms. Another common feature for all the investigated *R*–Ti–Sb systems is the negligible solubility of the third component in the binary compounds, except for the solubility of titanium in GdSb established here.

In the related *R*–{Zr, Hf}–Sb systems, the series of isotypic compounds R_3ZrSb_5, R_3HfSb_5 (*R* = La-Nd, Sm) with Hf_5CuSn_3-type structure and *R*ZrSb (*R* = Y, Gd-Tm, Lu) with tetragonal CeScSi-type structure [36] group the only known ternaries. It appears that for the formation of compounds with stoichiometry R_3MSb_5 the size factor is decisive because these compounds are formed with *M* = Ti, Zr, and Hf, but only with early lanthanides. The structure of *R*ZrSb

(UGeTe-type) can be described as a superstructure of the binary La_2Sb structure type [37], in which the rare-earth metal atoms in Wyckoff position 4*c* (space group *I*4/*mmm*) have been replaced by transition metal atoms.

The crystal structures of the $R_2Ti_7Sb_{12}$ (R = La-Nd) and $R_2Ti_{11}Sb_{14}$ (R = Sm, Gd, Tb, Yb) compounds are similar in several aspects. First of all, the similarity is evident through the formation of a complex Ti-Sb networks in both cases. In both structures, these networks outline channels along the shortest unit cell dimension (*c* for $R_2Ti_7Sb_{12}$ and *b* for $R_2Ti_{11}Sb_{14}$), which are occupied by rare-earth metal atoms (in $R_2Ti_7Sb_{12}$, the channels are also occupied by Sb atoms). As already suggested by Bie and Mar [11], the size of the R atom seems to be decisive for the formation of these two series of compounds. The interatomic distances in $R_2Ti_{11}Sb_{14}$ are significantly shorter than in $R_2Ti_7Sb_{12}$, and the structure itself looks more contracted, which may be the reason why the attempts to synthesize $R_2Ti_{11}Sb_{14}$ phases with the latest rare-earth metals failed. It may also explain the partial substitution of Ti by Sb observed in the compounds with Tb and Yb; this is due to the slightly larger size of the Sb atoms and can be seen as a reaction against the general contraction of the structure. Some interatomic distances in these structures are significantly shorter than the calculated sum of the atomic radii of the elements [38], which indicates prevalent covalent bonding. Possible local ordering among the partially occupied sites has been proposed [5,11], but this does not mean that the ordering in neighboring chains is correlated, and the overall structures generally remain disordered. Another peculiar feature of these structures is the formation of infinite columns of atoms of one element along the crystallographic direction that corresponds to the shortest unit cell parameter.

Conclusions

The phase equlibria in the ternary Ce–Ti–Sb and Gd–Ti–Sb systems were investigated and isothermal sections of the phase diagrams at 600°C were constructed for the first time. The systems are characterized by the formation of a small number of ternary compounds and negligible solubilities of the third component in the binary phases. Complete structure refinements were performed for the $Ce_2Ti_7Sb_{12}$ and $Gd_2Ti_{11}Sb_{14}$ compounds, confirming the earlier assigned structure types. The crystal structures are relatively complex and need further investigation. The formation of the Ti_5Sb_8 phase was confirmed in the Ti–Sb system.

Acknowledgements

This work was carried out under the grant of the Ministry of Education and Science of Ukraine No. 0115U003257.

References

[1] P. Villars, K. Cenzual, J. L. C. Daams, F. Hulliger, T. B. Massalski, H. Okamoto, K. Osaki, A. Prince, S. Iwata, *Pauling File. Inorganic Materials Database and Design System*. Binaries Edition, Crystal Impact, Bonn, 2001.
[2] P. Villars, K. Cenzual (Eds.), *Pearson's Crystal Data. Crystal Structure Database for Inorganic Compounds*, Release 2014/15, ASM International, Materials Park (OH), 2014.
[3] Y. Zhu, H. Kleinke, *Z. Anorg. Allg. Chem*. 628 (2002) 2233.
[4] H. Kleinke, *Inorg. Chem*. 40 (2001) 95-100.
[5] H. Bie, S.H.D. Moore, D.G. Piercey, A.V. Tkachuk, O.Y. Zelinska, A. Mar, *J. Solid State Chem*. 180 (2007) 2216-2224.
[6] A. Kjekshus, F. Gronvold, J. Thorbjornsen, *Acta Chem. Scand*. 16 (1962) 1493-1510.
[7] S. Bobev, H. Kleinke, *Chem. Mater*. 15 (2003) 3523-3529.
[8] H. Wu, A.V. Skripov, T.J. Udovic, J.J. Rush, S. Derakhshan, H. Kleinke, *J. Alloys Compd*. 496 (2010) 1-6.
[9] G. Bollore, M.G. Ferguson, R.W. Hushagen, A. Mar, *Chem. Mater*. 7 (1995) 2229-2231.
[10] S.H.D. Moore, L. Deakin, M.G. Ferguson, A. Mar, *Chem. Mater*. 14 (2002) 4867-4873.
[11] H. Bie, A. Mar, *Inorg. Chem*. 47 (2008) 6763-6770.
[12] W. Rieger, H. Nowotny, F. Benesowsky, *Monatsh. Chem*. 96 (1965) 232-241.
[13] A. Guzik, *J. Alloys Compd*. 423 (2006) 40-42.
[14] J. Nuss, H.G. Von Schnering, *Z. Kristallogr. - New Cryst. Struct*. 217 (2002) 21.
[15] O.V. Zhak, O.V. Pugach, Y.B. Kuzma, *Visn. Lviv. Nat. Univ., Ser. Khim*. 43 (2003) 15-20.
[16] R. Nirmala, A.V. Morozkin, O. Isnard, A.K. Nigam, *J. Magn. Magn. Mater*. 321 (2009) 188-191.
[17] V.D. Abulkhaev, *Russ. J. Inorg. Chem*. 42 (1997) 283-286.
[18] S. Gupta, E.A. Leon Escamilla, F. Wang, G.J. Miller, J. D. Corbett, *Inorg. Chem*. 48 (2009) 4362-4372.
[19] Y.Y. Janice Cheung, V.O. Svitlyk, Y. Mozharivskyj, *Inorg. Chem*. 51 (2012) 10169-10175.
[20] V.Y. Gvozdetskii, N.V. German, R.E. Gladyshevskii, *Visn. Lviv. Nat. Univ., Ser. Khim*. 53 (2012) 12-19.

[21] N.L. Eatough, H. T. Hall, *Inorg. Chem*. 8 (1969) 1439-1445.
[22] G. Borzone, M.L. Fornasini, N. Parodi, R. Ferro, *Intermetallics* 8 (2000) 189-194.
[23] W. Jeitschko, R.O. Altmeyer, M. Schelk, U.C. Rodewald, *Z. Anorg. Allg. Chem*. 627 (2001) 1932-1940.
[24] S. Ramakrishnan, G. Chandra, *Phys. Lett.* 100 (1984) 441-444.
[25] S. Derakhshan, A. Assoud, K.M. Kleinke, E. Dashjav, X. Qiu, S.J.L. Billinge, H. Kleinke, *J. Am. Chem. Soc*. 126 (2004) 8295-8302.
[26] G.A. Melnyk, W. Tremel, *J. Alloys Compd*. 349 (2003) 164-171.
[27] J.W. Kaiser, M.G. Haase, W. Jeitschko, *Z. Anorg. Allg. Chem*. 627 (2001) 2369-2376.
[28] A.Y. Kozlov, V.V. Pavlyuk, *J. Alloys Compd*. 367 (2004) 76-79.
[29] M. Armbrüster, W. Schnelle, U. Schwarz, Y. Grin, *Inorg. Chem*. 46 (2007) 6319-6328.
[30] H. Kleinke, *Can. J. Chem.* 79 (2001) 1338-1343.
[31] STOE WinXPOW, version 3.03. Stoe & CieGmbH, Darmstadt, Germany, 2010.
[32] T. Holland, S. Redfern, *Mineralog. Mag.* 61 (1997) 65-77.
[33] J. Rodríguez-Carvajal, *Commission on Powder Diffraction* (*IUCr*), *Newsletter*. 26 (2001) 12-19.
[34] O. Senchuk, Ya. Tokaychuk, P. Demchenko, R. Gladyshevskii, *Coll. Abstr. XIII Int. Conf. Cryst. Chem. Intermet. Compd*., Lviv, Ukraine, 2016, p. 69.
[35] O. Senchuk, Ye. Starokon', Ya. Tokaychuk, P. Demchenko, R. Gladyshevskii, *Coll. Abstr. XIII Int. Conf. Cryst. Chem. Intermet. Compd*., Lviv, Ukraine, 2016, p. 70.
[36] A.V. Morozkin, I.A. Sviridov, *J. Alloys Compd*. 320 (2001) L1-L2.
[37] W.N. Stassen, M. Sato, L.D. Calvert, *Acta Cryst. B* 26 (1970) 1534-1540.
[38] J. Emsley, *The Elements. Second Edition*, Clarendon Press, Oxford, 1991, 256 p.